Materials Advances

ROYAL SOCIETY OF CHEMISTRY

COMMUNICATION

View Article Online
View Journal | View Issue

Check for updates

Cite this: *Mater. Adv.*, 2022, 3, 6988

Received 20th May 2022,
Accepted 9th August 2022

DOI: 10.1039/d2ma00566b

rsc.li/materials-advances

Swimming protein microtube motors capture virus-shaped fluorescent nanoparticles†

Yushi Akashi, Natsuho Sugai, Ryo Kato and Teruyuki Komatsu *

Hemagglutinins (HAs), spike proteins of influenza virus, were fixed on luminous polystyrene beads to make HA-immobilized fluorescent nanoparticles (HA-FNPs). The protein MTs with an exterior surface of fetuin and an interior surface of catalase (Fet/Cat MTs) were self-propelled in aqueous H_2O_2 solution by spouting O_2 bubbles. They captured molecular HAs and virus-shaped HA-FNPs efficiently.

Influenza viruses are annoying pathogens for human beings. Thucydides reported an infectious disease that struck Athens in 430 B.C. Presumably, that is the earliest recorded outbreak of what we know as influenza.[1] Among the three influenza virus types of A, B and C, type A tends to engender severe diseases.[2] It belongs to the *Orthomyxoviridae* family, with a negative-sense single-stranded RNA genome. In 2009, swine-origin A (H1N1) virus caused a human pandemic.[3] The initial infection of influenza A virus starts from the specific binding of spike protein hemagglutinin (HA) to a cellular surface receptor containing sialyl oligosaccharide with *N*-acetyl neuraminic acid (Neu5Ac) terminuses.[4] Currently, great interest has arisen in the study of infectious viral particles. It is nonetheless difficult to handle these pathogens in a common experimental laboratory. Moreover, analyses of viruses must be sensitive. To develop virus research extensively, we created a non-infectious and highly detectable fake virus, an HA-immobilized fluorescent nanoparticle (HA-FNP), on which the HAs are fixed by Ni-histidine (His)-tag complexation. The functionality of HA coordinated on the particle has been changed as little as possible. Swimming cylindrical motors of micrometer size with autonomous propulsion have attracted considerable attention because of their versatility, with diverse potential applications[5–24] that include as drug carriers,[12,14,17,18,20] environmental remediators,[13,21,24] and analytical sensors.[22,23] One beneficial procedure to synthesize these hollow swimmers is template synthesis using layer-by-layer (LbL) assembly in a track-etched polycarbonate (PC) membrane.[12,14,16,17,20,24] Such fabricated unique microtube (MT) motors able to capture influenza viruses would strongly benefit not only nanomaterials science, but also diagnostic applications. Fetuin from fetal calf serum (Fet, M_w: 48.4 kDa, pI: 3.3), a glycosylated protein with tribranched oligosaccharides containing Neu5Ac residues,[25] interacts with influenza viruses.[26,27] This paper is the first to describe the synthesis of catalase (Cat)-driven protein MT motors with a fetuin layer as an external wall and to explain their efficient capture of molecular HAs and spherical HA-FNPs.

The stratiform Fet/PLA/HSA/MNP(PLA/HSA)$_5$PLA/PLG/Avi/bCat MTs (Fet/Cat MTs) were prepared using our earlier reported procedures of LbL assembly using a PC membrane template [PLA, poly(L-arginine); HSA, human serum albumin; MNP, magnetite nanoparticle; PLG, poly(L-glutamic acid); Avi, avidin; bCat, biotinylated catalase] (Fig. 1).[24] Phosphate buffered (PB) solution of Fet was added to decorate the outer surface of the precursor PLA/HSA/MNP(PLA/HSA)$_5$PLA/PLG/Avi/bCat MTs (Cat MTs), yielding the designed Fet/Cat MTs. The transmission electron microscopy (TEM) images of the air-dried sample revealed that the MTs swelled considerably in water. They had 1.15 μm outer diameter and 24 μm tube length. The wall thickness was 281 nm (Fig. 2A). The Fet coverage rate of the tube surface was ascertained using fluorescent Cy5.5-labeled Fet (CyFet). After centrifugation of the mixture of Cat MTs and CyFet, the fluorescence intensity of the supernatant was 33% of that observed for the identically treated CyFet solution without the tubes. This result signifies that the number of adhered CyFet molecules onto one tube was approximately 3.9×10^6 per tube. Thereby, the coverage rate of the MT surface with CyFet was estimated as 58%. Similar tubules have been produced using fluorescein-labeled Cat (FCat) as an

Department of Applied Chemistry, Faculty of Science and Engineering, Chuo University, 1-13-27 Kasuga, Bunkyo-ku, Tokyo 112-8551, Japan.
E-mail: komatsu@kc.chuo-u.ac.jp

† Electronic supplementary information (ESI) available: Detailed experimental procedures; the fluorescence spectra of HA-FNP solution after treatment with self-propelled Fet/Cat MT motors (Fig. S1); the TEM image of HA-FNP bound Fet/Cat MT (Fig. S2) (all PDF); self-propelled motion of a Fet/Cat MT motor (Video S1) (AVI); self-propelled motion of a FIgG-HA-Fet/Cat MT motor (Video S2) (AVI); self-propelled motion of a HA-FNP bound Fet/Cat MT motor (Video S3) (AVI). See DOI: https://doi.org/10.1039/d2ma00566b

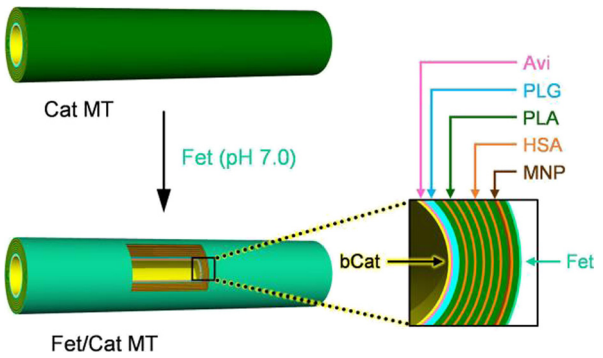

Fig. 1 Preparation and stratiform structure of the protein MT motor with a Cat engine layer as an internal wall and Fet exterior surface: Fet/PLA/HSA/MNP(PLA/HSA)$_5$PLA/PLG/Avi/bCat MT (Fet/Cat MT).

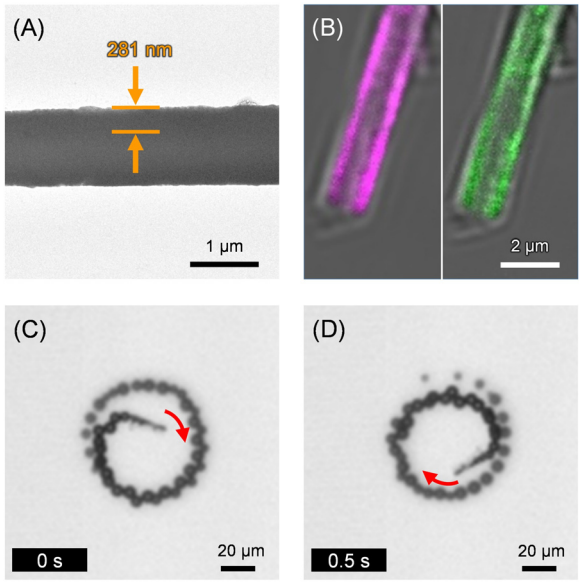

Fig. 2 (A) The TEM image of Fet/Cat MT. (B) The CLSM images of CyFet/FCat MT (left – λ_{ex}, 633 nm for CyFet; right – λ_{ex}, 488 nm for FCat). (C and D) Snapshots taken from Video S1 (ESI†) of microscopic observations of self-propelled Fet/Cat MT by ejecting O_2 bubbles in PB solution (pH 7.0, 2 wt% H_2O_2, and 0.1 wt% Triton X-100) at 25 °C under bright field mode.

internal wall. The CLSM images of the CyFet/FCat MTs showed both fluorescence colors (Fig. 2B), implying that the FCat molecules are adhered on the interior wall and that the CyFet molecules are bound onto the exterior surface of the hollow cylinder. The Fet/Cat MTs were self-propelled in aqueous H_2O_2 solution by ejecting O_2 bubbles from the open end terminus with an average velocity of 64 ± 5 μm s^{-1} (2.7 body-lengths per s) (pH 7.0, 2 wt% H_2O_2, and 0.1 wt% Triton X-100) (Fig. 2C and D and Video S1, ESI†). The swimming behavior of Fet/Cat MT was similar to that of the parent Cat MT.[16]

After HA solution was added to the PB dispersion of self-propelled Fet/Cat MTs (pH 7.0, 2 wt% H_2O_2, and 0.1 wt% Triton X-100), the mixture was left for 15 min without vibration in the dark at 25 °C. By bringing a Nd-magnet closer to the cuvette, the HA bound Fet/Cat MTs (HA-Fet/Cat MTs) were attracted to the bottom. The supernatant was analyzed using direct enzyme-linked immunosorbent assay (ELISA) to ascertain the concentration of the unbound free HA. The HA concentration was only 8% of that observed for the identically treated HA without the Fet/Cat MTs (Fig. 3A). This result indicated that 92% of HA was removed from the sample solution by a single treatment with the swimming MTs. This finding enables us to calculate the average number of HA molecules absorbed onto one tubule as 1.2×10^6 per tube.

To clarify that the fetuin surface of the tube indeed captures the HA, identical experiments were conducted using similar MTs: HSA/PLA/HSA/MNP(PLA/HSA)$_5$PLA/PLG/Avi/bCat MTs (HSA/Cat MTs). Incubation with the HSA/Cat MTs, in which HSA was used instead of Fet, showed only 5% reduction of the HA amount (Fig. 3A). Furthermore, incubation with the non-swimming Fet/PLA/HSA/MNP(PLA/HSA)$_5$PLA/PLG MTs (Fet/PLG MTs) decreased 3% relative to the control value. Our results proved that self-propelled Fet/Cat MTs capture HA efficiently and that their motion plays an important role in accelerating the contact frequency to catch the HA.

To ensure HA binding onto the Fet surface, we used fluorescent anti-hemagglutinin IgG antibody (FIgG). Upon addition of FIgG to the PB solution of the swimming HA-Fet/Cat MTs (pH 7.0, 2 wt% H_2O_2, and 0.1 wt% Triton X-100), the antibody adhered immediately on the tubes' exterior surface. Optical microscopy observation under fluorescence mode revealed that the swimming FIgG-bound HA-Fet/Cat MTs (FIgG-HA-Fet/Cat MTs) emitted green fluorescence (Fig. 3B–D and Video S2, ESI†). The average velocity was 71 ± 9 μm s^{-1} (3.0 body-lengths per s). In light of these findings, we inferred that (i) specific interaction between HA and the sialyl oligosaccharide chain of the Fet wall is responsible for HA capture and that (ii) propulsion is crucially important to promote HA capture.

Next, we investigated the capture of virus-shaped fluorescent NPs with the swimming Fet/Cat MT motors. Moulès *et al.* reported the morphology of the influenza A virus [Puerto Rico/8/34 (PR8, H1N1)] virion using cryogenic TEM (cryoTEM).[28] The PR8 viruses comprised a mixture of spherical particles (94 ± 15 nm diameter) and elongated particles. We chose carboxylated fluorescent polystyrene NPs (FNPs, 100 nm diameter) as a luminous core. First, Ni^{2+}-nitrilotriacetic acid (Ni-NTA) groups were introduced onto the FNP surface (Scheme 1). Subsequently, the HA having a His-tag was complexed with the Ni-NTA groups on the bead, thereby yielding HA-FNPs. After dialysis of the mixture, the HA concentration in the external dialysate was negligible, as revealed by ELISA; the amount was below the detection limit. We inferred that all HA molecules bound to the particle as a spike protein in our experimental protocol. The number of HAs on one NP was ascertained as approximately 400, which is equivalent to the value of the natural influenza A virus.[28] TEM observation clearly revealed a monomolecular HA layer with 10 nm thickness on the particles (Fig. 4A). The positive contrast of HA can be attributed to uranyl acetate (UO^{2+}) staining. An earlier report described that this negative contrasting agent works as a positive staining material

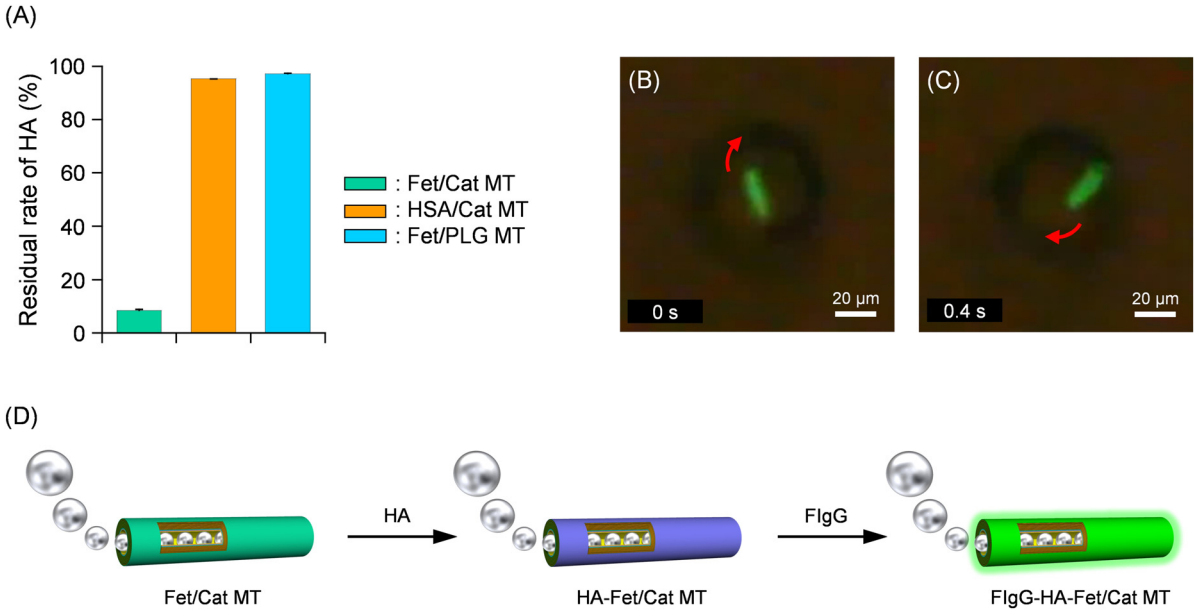

Fig. 3 (A) Residual rate of HA after incubation with self-propelled Fet/Cat MTs. (B and C) Snapshots taken from Video S2 (ESI†) of microscopic observations of self-propelled FIgG bound HA-Fet/Cat MT by spouting O_2 bubbles in PB solution (pH 7.0, 2 wt% H_2O_2, and 0.1 wt% Triton X-100) at 25 °C under fluorescence mode. (D) Schematic illustration of HA capture and subsequent FIgG binding on the exterior surface of a bubble-propelled Fet/Cat MT.

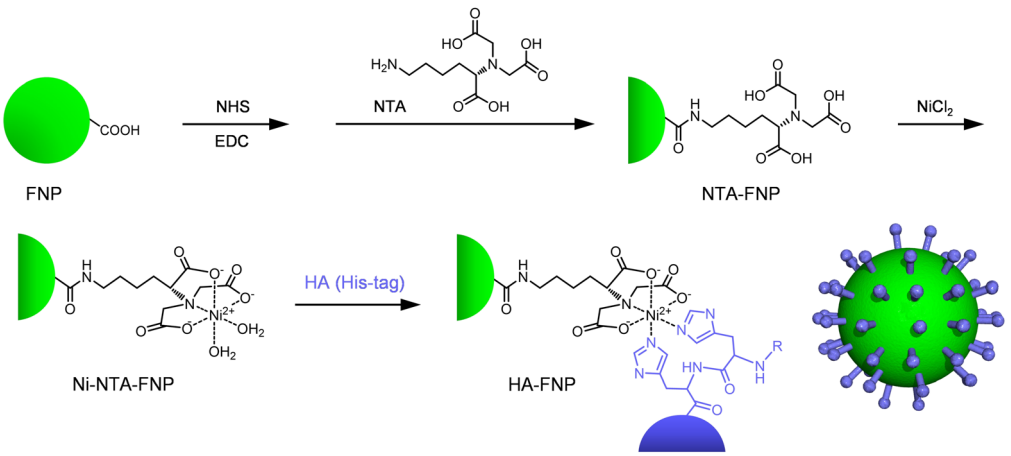

Scheme 1 Synthetic route of HA-FNPs.

for certain proteins.[29] This reverse effect caused the dark image of the HAs. Several different methods are currently available to characterize the nanostructure of protein-immobilized particles.[30] However, the detailed physicochemical features of the HA-FNP surface are not very important at this stage. This will be revealed in the near future. The luminous HA-FNPs are a non-infectious fake influenza A virus, which can be detected with high sensitivity using fluorescence spectroscopy.

Later, the HA-FNPs were injected into the PB dispersion of self-propelled Fet/Cat MTs. The mixture (pH 7.0, 2 wt% H_2O_2, and 0.1 wt% Triton X-100) was left for 2 h without vibration in the dark at 25 °C. Using a Nd-magnet, the HA-FNP-bound Fet/Cat MTs were removed carefully. As expected, the fluorescence intensity of the supernatant was only 54% of that of the control solution without the tubes (Fig. S1A, ESI†). It became apparent that *ca.* 2.0×10^3 particles bound to one tube (Fig. 4B). The swimming Fet/Cat MTs with bound HA-FNP fluoresced strongly; their velocity was 72 ± 8 μm s^{-1} (3.0 body-lengths per s) (Fig. 4C and Video S3, ESI†). It is noteworthy that the HA-FNPs were absorbed tightly onto the Fet exterior wall. The HA binding to the Fet layer is sufficiently strong to retain the NPs, which were never released. Subsequent TEM observations indicated definitively that HA-FNPs were immobilized onto the cylindrical surface (Fig. S2, ESI†). The image shows the particles absorbed on both sides of the flattened tube as 2.0×10^3 pieces (85 pieces per μm-tube-length), which is exactly

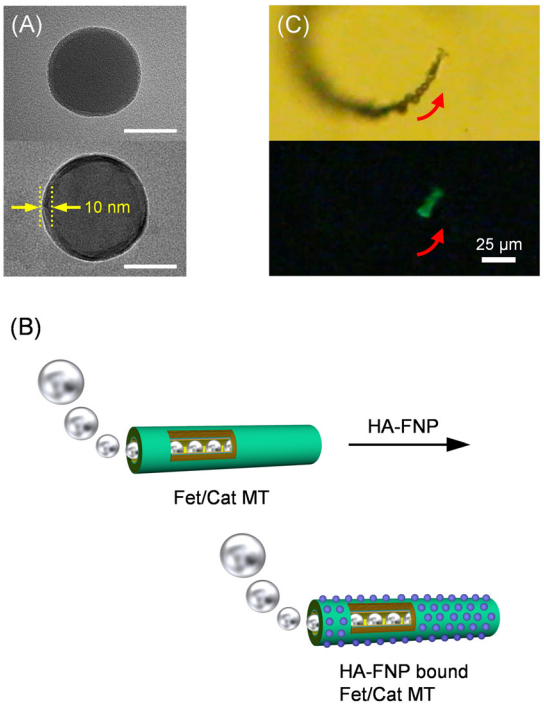

Fig. 4 (A) TEM images of (top) unmodified FNPs and (bottom) HA-FNPs (bar: 50 nm). (B) Schematic illustration of HA-FNPs capturing a bubble-propelled Fet/Cat MT. (C) Snapshots taken from Video S3 (ESI†) of microscopic observations of self-propelled HA-FNP bound Fet/Cat MT by ejecting O_2 bubbles in PB solution (pH 7.0, 2 wt% H_2O_2, and 0.1 wt% Triton X-100) at 25 °C under (top) bright field mode and (bottom) fluorescence mode.

equal to the value obtained from the fluorescence measurements. By contrast, when adding Ni-NTA-FNPs instead of HA-FNPs, the fluorescence change was negligibly small (Fig. S1B, ESI†). This finding implies that Fet/Cat MT motors recognize the HA surface of the particle.

In conclusion, Cat-driven MT motors composed of blood serum proteins (HSA and fetuin) captured influenza virus-shaped FNPs, which can be used easily in a normal laboratory without restriction. This system involves no antigen–antibody reaction. Therefore, virus-shaped FNPs of various kinds can be created using His-tagged spike proteins of desired viruses and different size fluorescent NPs. These particles are expected to be effective for virus research in common laboratory environments. The swimming Fet/Cat MTs might be applicable as detectors for several viruses. They are expected to be of diagnostic importance for use in advanced biotechnology.

This work was supported by Grants-in-Aid for Scientific Research (B) (No. 18H01833 and No. 21H01767) from JSPS.

Author contributions

T. K. designed and initiated this study. All the authors conducted experiments and analysed the data. Y. A., N. S. and T. K. drafted the manuscript.

Conflicts of interest

The authors declare no competing financial interest.

References

1 A. D. Langmuir, T. D. Worthen, J. Solomon, C. G. Ray and E. Peterson, *New Engl. J. Med.*, 1985, **313**, 1027–1030.
2 R. A. Medina and A. Garcia-Sastre, *Nat. Rev. Microbiol.*, 2011, **9**, 590–603.
3 H. V. Fineberg, *New Engl. J. Med.*, 2014, **370**, 1335–1342.
4 W. Weis, J. H. Brown, S. Cusack, J. C. Paulson, J. J. Skehel and D. C. Wiley, *Nature*, 1988, **333**, 426–431.
5 Y. Mei, G. Huang, A. A. Solovev, E. B. Ureña, I. Mönch, F. Ding, T. Reindl, R. K. Y. Fu, P. K. Chu and O. G. Schmidt, *Adv. Mater.*, 2008, **20**, 4085–4090.
6 W. Gao, S. Sattayasamitsathit, J. Orozco and J. Wang, *J. Am. Chem. Soc.*, 2011, **133**, 11862–11864.
7 Y. Mei, A. A. Solovev, S. Sanchez and O. G. Schmidt, *Chem. Soc. Rev.*, 2011, **40**, 2109–2119.
8 H. Wang and M. Pumera, *Chem. Rev.*, 2015, **115**, 8704–8735.
9 Z. Wu, X. Lin, T. Si and Q. He, *Small*, 2016, **12**, 3080–3093.
10 B. Xu, B. Zhang, L. Wang, G. Huang and Y. Mei, *Adv. Funct. Mater.*, 2018, **28**, 1705872.
11 M. Safdar, S. U. Khan and J. Jänis, *Adv. Mater.*, 2018, **30**, 1703660.
12 T. Komatsu, *Chem. Lett.*, 2020, **49**, 1245–1255.
13 L. Soler, V. Magdanz, V. M. Fomin, S. Sanchez and O. G. Schmidt, *ACS Nano*, 2013, **11**, 9611–9620.
14 Z. Wu, W. Lin, X. Zou, J. Sun and Q. He, *ACS Appl. Mater. Interfaces*, 2015, **7**, 250–255.
15 Y. Yoshizumi and H. Suzuki, *ACS Appl. Mater. Interfaces*, 2017, **9**, 21355–21361.
16 N. Sugai, Y. Nakai, Y. Morita and T. Komatsu, *ACS Appl. Nano Mater.*, 2018, **2**, 3080–3085.
17 Y. Nakai, N. Sugai, H. Kusano, Y. Morita and T. Komatsu, *ACS Appl. Nano Mater.*, 2019, **2**, 4891–4899.
18 B. Esteban-Fernández de Ávila, P. Angsantikul, X. Li, W. Gao, L. Zhang and J. Wang, *Adv. Funct. Mater.*, 2018, **28**, 1705640.
19 C. Liang, Z. Zhan, F. Zeng, D. Xu, Y. Wang, W. Zhao, J. Zhang, J. Guo, H. Feng and X. Ma, *ACS Appl. Mater. Interfaces*, 2018, **10**, 35099–35107.
20 W. Wang, Z. Wu, X. Lin, T. Si and Q. He, *J. Am. Chem. Soc.*, 2019, **141**, 6601–6608.
21 X. Bing, X. Zhang, J. Li, D. H. L. Ng, W. Yang and J. Yang, *J. Mater. Chem. A*, 2020, **8**, 2809–2819.
22 C. C. Mayorga-Martinez and M. Pumera, *Adv. Funct. Mater.*, 2020, **30**, 1906449.
23 Á. Molinero-Fernández, M. Á. López and A. Escarpa, *Anal. Chem.*, 2020, **92**, 5048–5054.
24 M. Umebara, N. Sugai, K. Murayama, T. Sugawara, Y. Akashi, Y. Morita, R. Kato and T. Komatsu, *Mater. Adv.*, 2021, **2**, 6428–6438.
25 W. M. Brown, N. R. Saunders, K. Mollgard and K. M. Dziegielewska, *BioEssays*, 1992, **14**, 749–755.
26 D. K. Takemoto, J. J. Skehel and D. C. Wiley, *Virology*, 1996, **217**, 452–458.

27 B. Meng, A. C. Marriott and N. J. Dimmock, *Influenza Other Respir. Viruses*, 2010, **4**, 147–153.
28 V. Moulès, O. Terrier, M. Yver, B. Riteau, C. Moriscot, O. Ferraris, T. Julien, E. Giudice, J.-P. Rolland, A. Erny, M. Bouscambert-Duchamp, E. Frobert, M. Rosa-Calatrava, Y. P. Lin, A. Hay, D. Thomas, G. Schoehn and B. Lina, *Virology*, 2011, **414**, 51–62.
29 X. Qu and T. Komatsu, *ACS Nano*, 2010, **4**, 563–573.
30 P. M. Kelly, C. Åberg, E. Polo, A. O'Connell, J. Cookman, J. Fallon, Ž. Krpetić and K. A. Dawson, *Nat. Nanotechnol.*, 2015, **10**, 472–479.